DOI: 10.1002/chem.200800595

Biomimetic Iron-Catalyzed Asymmetric Epoxidation of Aromatic Alkenes by Using Hydrogen Peroxide

Feyissa Gadissa Gelalcha,*[a] Gopinathan Anilkumar,[b] Man Kin Tse,[c] Angelika Brückner,[c] and Matthias Beller*[c]

Abstract: A novel and general biomimetic non-heme Fe-catalyzed asymmetric epoxidation of aromatic alkenes by using hydrogen peroxide is reported herein. The catalyst consists of ferric chloride hexahydrate ($FeCl_3 \cdot 6H_2O$), pyridine-2,6-dicarboxylic acid (H_2-(pydic)), and readily accessible chiral *N*-arenesulfonyl-*N*′-benzyl-substituted ethylenediamine ligands. The asymmetric epoxidation of styrenes with this system gave high conversions but poor enantiomeric excesses (*ee*), whereas larger alkenes gave high conversions and *ee* values. For the epoxidation of *trans*-stilbene (**1a**), the ligands (*S*,*S*)-*N*-(4-toluenesulfonyl)-1,2-diphenylethylenediamine ((*S*,*S*)-**4a**) and its *N*′-benzylated derivative ((*S*,*S*)-**5a**) gave opposite enantiomers of *trans*-stilbene oxide, that is, (*S*,*S*)-**2a** and (*R*,*R*)-**2a**, respectively. The enantioselectivity of alkene epoxidation is controlled by steric and electronic factors, although steric effects are more dominant. Preliminary mechanistic studies suggest the in situ formation of several chiral Fe-complexes, such as [FeCl(L*)$_2$-(pydic)]·HCl (L* = (*S*,*S*)-**4a** or (*S*,*S*)-**5a** in the catalyst mixture), which were identified by ESIMS. A UV/Vis study of the catalyst mixture, which consisted of $FeCl_3 \cdot 6H_2O$, H_2(pydic), and (*S*,*S*)-**4a**, suggested the formation of a new species with an absorbance peak at $\lambda =$ 465 nm upon treatment with hydrogen peroxide. With the aid of two independent spin traps, we could confirm by EPR spectroscopy that the reaction proceeds via radical intermediates. Kinetic studies with deuterated styrenes showed inverse secondary kinetic isotope effects, with values of $k_H/k_D = 0.93$ for the β carbon and $k_H/k_D = 0.97$ for the α carbon, which suggested an unsymmetrical transition state with stepwise O transfer. Competitive epoxidation of *para*-substituted styrenes revealed a linear dual-parameter Hammett plot with a slope of 1.00. Under standard conditions, epoxidation of **1a** in the presence of ten equivalents of $H_2{}^{18}O$ resulted in an absence of the isotopic label in (*S*,*S*)-**2a**. A positive nonlinear effect was observed during the epoxidation of **1a** in the presence of (*S*,*S*)-**5a** and (*R*,*R*)-**5a**.

Keywords: asymmetric catalysis · epoxidation · hydrogen peroxide · iron · radical reactions

Introduction

Optically active oxiranes represent key building blocks for the synthesis of fine chemicals and pharmaceuticals.[1] Catalytic asymmetric epoxidation represents an interesting tool for their synthesis as an alternative to the more common kinetic resolution processes.[2] In this regard, the state-of-the-art protocols are the Sharpless epoxidation of allylic alcohols with titanium tartarate complexes;[3] the Katsuki–Jacobsen epoxidation of unfunctionalized alkenes by using chiral [Mn{*N*,*N*′-bis(salicylidene)ethylenediamine}] catalysts;[4] organocatalytic methods that utilize chiral ketone catalysts, as pioneered by Shi et al.;[5] and the Julia epoxidation of enones by using poly-L-leucine with bases as the catalysts.[6] The development of less expensive and environmentally more benign catalysts and oxidant systems that have a wider

[a] Dr. F. G. Gelalcha
4900 East University Boulevard, 609
Odessa, Texas 79762 (USA)
E-mail: fgadissa@yahoo.de

[b] Dr. G. Anilkumar
Anthem Biosciences Pvt Ltd
49 Canara Bank Road
Bangalore 560 099 (India)

[c] Dr. M. K. Tse, Dr. A. Brückner, Prof. Dr. M. Beller
Leibniz-Institut für Katalyse e.V. an der Universität Rostock
Albert Einstein Strasse 29a
18059 Rostock (Germany)
Fax: (+49) 381-12815000
E-mail: matthias.beller@catalysis.de

Supporting information for this article is available on the WWW under http://www.chemeurj.org/ or from the authors.

scope of applicability remains a challenge in organic synthesis. Hydrogen peroxide is one of the most practical terminal oxidants in terms of cost and atom efficiency. In recent years, this oxidant has become increasingly popular in organocatalytic oxidations[7] and in metal-catalyzed asymmetric epoxidations.[8] Thus, Ti-,[9] Pt-,[10] and Ru-based catalysts[11] have been reported for asymmetric epoxidations of olefins by using hydrogen peroxide. Similarly, iron is a cheap, versatile, and less toxic catalyst.[12] Indeed, a highly efficient, though impractical, biomimetic asymmetric epoxidation of styrene derivatives has been developed recently, which uses iodosobenzene in dichloromethane as the oxidant and chiral iron porphyrin complexes.[13] Similarly, the aerobic asymmetric epoxidation of styrene derivatives, which is catalyzed by a tris(D,D-dicampholylmethanato) iron(III) complex ([Fe(dcm)$_3$]) and uses sacrificial reductant and a chlorinated solvent,[14] the asymmetric epoxidation of *trans*-methylstyrene by employing Fe complexes with peptidelike ligands as the catalysts,[15] and the iron-catalyzed asymmetric peracid epoxidation of electron-poor alkenes[16] have been described. All of these methods are less attractive from a practical point of view.

Recently, we reported the first breakthrough and a promising non-heme iron-catalyzed asymmetric epoxidation of aromatic alkenes by using hydrogen peroxide, which not only gives good-to-excellent isolated yields of epoxides but also enantiomeric excess (*ee*) values of up to 97%.[17] Herein, we report on the further extension of this novel catalytic asymmetric epoxidation system to more commonly encountered alkenes, preliminary mechanistic insights, and give a full account of experimental details of the reaction.

Results and Discussion

Ligand design and substrate scope: As stated previously, we have investigated the epoxidation of *trans*-stilbene (**1a**) to *trans*-stilbene oxide (**2a**) by using 30% hydrogen peroxide as the oxidant. Our catalyst systems consisted of commercially available iron salts (such as ferric chloride hexahydrate), pyridine-2,6-dicarboxylic acid (H_2(pydic)), and carefully chosen chiral *N*-sulfonylated ethylene diamine derivatives.[17] The required ligands are easily accessible by the monosulfonylation of optically pure C_2-symmetrical 1,2-diamines, such as (−)-(*S,S*)-1,2-diphenylethylenediamine (**3**), with arenesulfonylchlorides in the presence of bases, such as diisopropyl ethylamine (DIPEA), and, where necessary, reductive *N*-alkylation of the resulting products (**4**) in the presence of suitable aldehydes and sodium borohydride ($NaBH_4$; Scheme 1). The influence of various ligands **4** and **5** on the enantioselectivity of the reaction is summarized in Table 1.

The observation that the commercially available ligand (*S,S*)-*N*-(4-toluenesulfonyl)-1,2-diphenylethylenediamine ((*S,S*)-TsDPEN; (*S,S*)-**4a**) gave (−)-(2*S*,3*S*)-**2a** in 28% *ee* at room temperature (Table 1, entry 1) is in stark contrast with the racemic product observed when the unsubstituted ligand

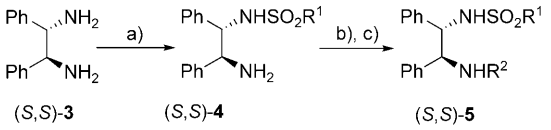

(*S,S*)-**3** (*S,S*)-**4** (*S,S*)-**5**

Scheme 1. General synthesis of optically pure substituted diphenylethylenediamine ligands. a) R^1SO_2Cl, DIPEA, CH_2Cl_2, 0°C–RT; b) ArCHO, EtOH, reflux; c) $NaBH_4$, EtOH, RT. See Table 1 for details of R^1 and R^2.

Table 1. Iron-catalyzed asymmetric epoxidation of **1a** by using (*S,S*)-**4a–c** and (*S,S*)-**5a–d**.[a]

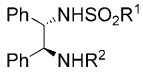

Entry	Compound	Ligand R^1	Ligand R^2	Conv[b] [%]	Yield[b] [%]	*ee*[c] [%], abs conf[d]
1	(*S,S*)-**4a**	4-MeC_6H_4	H	100	86	28, (−)-(2*S*,3*S*)
2	(*S,S*)-**4b**	4-PhC_6H_4	H	100	84	29, (−)-(2*S*,3*S*)
3	(*S,S*)-**4c**	4-*t*BuC_6H_4	H	100	84	29, (−)-(2*S*,3*S*)
4	(*S,S*)-**5a**	4-MeC_6H_4	Bn	100	87	42, (+)-(2*R*,3*R*)
5	(*S,S*)-**5b**	4-PhC_6H_4	Bn	100	84	39, (+)-(2*R*,3*R*)
6	(*S,S*)-**5c**	4-*t*BuC_6H_4	Bn	100	95	40, (+)-(2*R*,3*R*)
7	(*S,S*)-**5d**	4-MeC_6H_4	4-MeBn	100	92	39 (+)-(2*R*,3*R*)

[a] Conditions: *trans*-stilbene (0.5 mmol), H_2O_2 (1.0 mmol), $FeCl_3 \cdot 6H_2O$ (5.0 mol%), H_2(pydic) (5.0 mol%), (*S,S*)-**4** or (*S,S*)-**5** (12 mol%), *tert*-amyl alcohol, RT, 1 h. [b] Conversion and yield determined by GC with dodecane as the internal standard; error ±1%. [c] The *ee* of **2a** was determined by HPLC on a chiral column; error ±1%. [d] Absolute configuration determined by comparing the sign of the optical rotation of the major enantiomer with known data. Optical rotations were measured by using a chiral detector connected to a chiral HPLC.[18]

(*S,S*)-**3** is used as the chiral source. This led us to systematically modify the ligand to produce a sterically diverse set of structures, such as (*S,S*)-**4b,c** and (*S,S*)-**5a–d** (Table 1). *N*-Benzylation of the remaining amino group generally resulted in further enhancement of the product *ee* values by about 10% (Table 1, entries 4–7). It is obvious that among these compounds the simple *N*-benzyl-substituted derivative (*S,S*)-**5a** ((*S,S*)-BnTsDPEN) led to the most significant increase in *ee* values and gave (+)-(2*R*,3*R*)-**2a** in 42% *ee* (Table 1, entry 4). It is also striking that the *N*′-sulfonylated amines ((*S,S*)-**4a–c**) and the corresponding *N*-benzyl-*N*′-sulfonylated ligands ((*S,S*)-**5a–d**) gave excesses of enantiomers with opposite absolute configurations. These results suggested the existence of several catalyst species, the importance of specific spatial orientation of the chiral ligand imposed by a rigid aromatic ring system, and the possible role of π–π interaction and hydrogen bonding in controlling enantioselectivities.

A surprising effect of the concentration of (*S,S*)-**5a** (i.e., [(*S,S*)-**5a**]) on substrate conversion and on the *ee* value of **2a** was observed, as detailed in Table 2. As expected, at a

Table 2. Effect of the concentration of (*S,S*)-**5a** on the *ee* of (*R,R*)-**2a**.

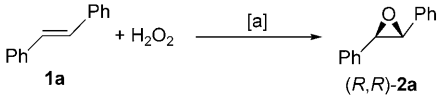

1a (*R,R*)-**2a**

Entry	(*S,S*)-**5a**[b] [mol%]	*t* [h]	Conv[c] [%]	Yield[c] [%]	*ee*[d] [%]
1	2.5	1	22	12	–[e]
2	2.5	16	71	52	38
3	5.0	1	64	48	–[e]
4	5.0	16	95	76	41
5	10.0	1	100	83	39
6	12.0	1	100	87	42
7	15.0	1	100	88	36
8	20.0	1	100	91	31

[a] Conditions: **1a** (0.5 mmol), H_2O_2 (30%, 1.0 mmol, 2 equiv), $FeCl_3{\cdot}6H_2O$ (5.0 mol%), H_2(pydic) (5.0 mol%), (*S,S*)-**5a**, *tert*-amyl alcohol (10 mL), RT. [b] Based on the substrate. [c] Conversion and yield determined by GC with dodecane as the internal standard. [d] The *ee* value of (*R,R*)-**2a** was determined by HPLC on a chiral column; the (+)-(2*R*,3*R*) enantiomer was the major product. [e] Not determined.

low [(*S,S*)-**5a**] of 2.5 mol%, low substrate conversion was observed after 1 h, whereas extending the reaction time to 16 h not only gave a higher conversion (71%) and yield (52%), but also resulted in a significant *ee* of 38% (Table 2, entries 1 and 2). By using only 5 mol% of (*S,S*)-**5a**, we could achieve an *ee* of 41% after 16 h although the conversion was not complete (95%). When the (*S,S*)-**5a** concentration was increased to 10 mol% the conversion was complete after only 1 h, although this did not change the *ee* significantly; the maximum *ee* value was observed with 12 mol% (*S,S*)-**5a**. Higher concentrations of (*S,S*)-**5a** (15 or 20 mol%; Table 2, entries 7 and 8) deteriorated the *ee* values without significantly altering the yields. This is of practical significant because avoiding high concentrations of catalyst is a positive contribution for the efficient use of resources and the current desire for the development of environmentally greener methodologies.

We have previously demostrated that, in the case of *trans*-stilbenes **1b–f** and **1h–i**, for a given substituent the catalyst activity increased on moving from the *ortho* to the *para* position of the substrate.[17] Thus, high enantioselectivities were obtained with sterically bulky 4,4′-dialkyl-substituted *trans*-stilbenes. The highest *ee* value (97%) was achieved with (*E*)-2-(4-*tert*-butylstyryl)naphthalene (**1j**), whereas **1k** gave a lower *ee* value. Therefore, we have extended the use of (*S,S*)-**5a** to the asymmetric epoxidation of more commonly encountered alkenes (Table 3).

It is obvious from Table 3 that the catalyst still displays considerable reactivity toward a wide range of alkenes. However, the enantioselectivities of small alkenes, such as the styrenes (Table 3, entries 1–7), are lower than those achieved with larger alkenes. Moreover, alkenes with similar steric demands (e.g., 4-chlorostyrene and 4-fluorostyrene versus 4-methylstyrene and 4-trifluoromethyl styrene) are oxidized with different enantioselectivities; this suggests that electronic effects are also important. Oxidation of cinnamyl alcohol gave the corresponding epoxide in 46% *ee* and 49% yield. Hydroxyl protection slightly reduced the yield and the *ee* value decreased to 29%. This suggested that hydrogen-bonding groups placed in appropriate positions could increase the *ee* values (Table 3, entries 8–10). *trans*-4,4′-Diisopropyl stilbene (**1g**) gave the epoxide in 71% *ee* (Table 3, entry 12), which is in agreement with the common trend

Table 3. Fe-catalyzed asymmetric epoxidation of aromatic alkenes.

(**1l-v**, **1g**) (**2l-v**, **2g**)

Entry	Alkene	Conv[b] [%]	Yield[b] [%]	*ee*[c] [%], Abs conf[d]
1	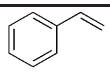 **1l**	100	84	8, –[e]
2	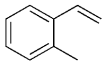 **1m**	100	61	8, –[e]
3	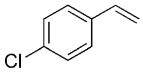 **1n**	100	82	21, (–)-(*R,R*)
4	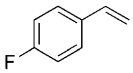 **1o**	100	73	11, –[e]
5	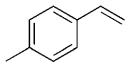 **1p**	100	52	26, –[e]
6	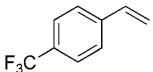 **1q**	72	60	20, –[e]
7	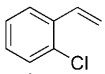 **1r**	91	62	14, –[e]
8	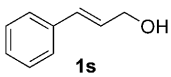 **1s**	100	49	48, (+)-(2*R*,3*R*)
9	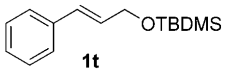 **1t**	100	42	29, (+)-(2*R*,3*R*)
10	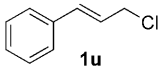 **1u**	57	33	23, (+)-(2*R*,3*R*)
11	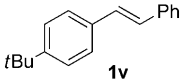 **1v**	100	91[f]	53, (+)-(2*R*,3*R*)
12	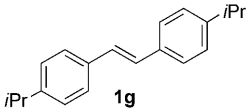 **1g**	100	90[f]	71, (+)-(2*R*,3*R*)

[a] Conditions: alkene (0.5 mmol), H_2O_2 (30%, 1.0 mmol, 2 equiv), $FeCl_3{\cdot}6H_2O$ (5.0 mol%), H_2(pydic) (5.0 mol%), (*S,S*)-**5a** (12 mol%), *tert*-amyl alcohol, RT, 1 h. TBDMS = *tert*-butyldimethylsilyl. [b] Conversion and yield determined by gas chromatography with dodecane as the internal standard. [c] Determined by HPLC on a chiral column. [d] Absolute configuration determined by comparing the sign of the optical rotation of the major enantiomer with known data. Optical rotations were measured by using a chiral detector connected to a chiral HPLC. See also ref. [19] for Entries 3 and 7, ref. [20] for Entry 8, ref. [21] for Entry 9, ref. [22] for Entry 10, and ref. [18] for Entry 12. [e] Not determined. [f] Isolated yield.

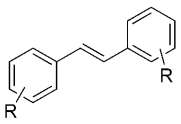

1b: R=2,2'-Me **1f**: R=3,3'-*i*Pr

1c: R=3,3'-Me **1g**: R=4,4'-*i*Pr

1d: R=4,4'-Me **1h**: R=3,3'-*t*Bu

1e: R=2,2'-*i*Pr **1i**: R=4,4'-*t*Bu

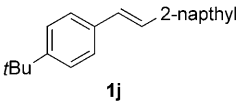

1j

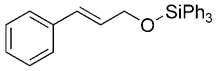

1k

previously observed for *trans*-4,4′-dialkyl-substituted stilbenes **1d** and **1i**.[17]

Preliminary mechanistic investigations

ESIMS studies: The ESI mass spectrum of the catalyst mixture ($FeCl_3$·6H_2O, 0.025 mmol; H_2(pydic), 0.025 mmol; (*S,S*)-**4a**, 0.06 mmol) in isopropanol/water (50:50, v/v)[23] is dominated by the signal of the chiral ligand (*S,S*)-**4a** ([*M*+H$^+$]; *m/z* 367.1484) and a signal that corresponds to its dimeric form $(TsDPEN)_2$ ([*M*+H$^+$]; *m/z* 733.28791). It also displays a complex set of very weak signals, which were assigned to various Fe-containing species: [Fe(pydic)TsDPEN]$^+$ ([*M*$^+$]; *m/z* 587.08394), [Fe$(pydic)_2$TsDPEN]$^+$ ([*M*$^+$]; *m/z* 953.22649), [FeCl(pydic)$(TsDPEN)_2$]·HCl+H$^+$ ([*M*+H$^+$]; *m/z* 1025.18204), and [Fe{H_2(pydic)}(pydic)$(TsDPEN)_2$]$^+$ ([*M*$^+$]; *m/z* 1120.249). An attempted crystallization of a pale yellow product that was isolated from the catalyst mixture, which consisted of $FeCl_3$·6H_2O, H_2(pydic), and (*S,S*)-**5a** in a ratio of 1:1:2.1 stirred in *tert*-amyl alcohol at room temperature for 2 h, failed. However, ESIMS analysis of this product revealed the presence of BnTsDPEN ([*M*+H$^+$]; *m/z* 457.3502) as the dominant species, together with a less intense signal that corresponds to the [Fe$(BnTsPDEN)_2$Cl(pydic)]·HCl ([*M*+H$^+$]; *m/z* 1205.2847) species, which is in full accordance with the calculated spectrum. Very small signals at *m/z* 1300.3287 and 1556.248, which correspond to as-yet uncharacterized Fe-containing species, were also detected. Both results suggest the formation of complex equilibria, which supports the hypothesis that a chiral Fe–ligand complex is responsible for the asymmetric induction. However, which of these precatalysts converts to the active catalyst upon treatment with hydrogen peroxide is currently under investigation.

UV/Vis spectroscopy: When a dilute solution of aqueous hydrogen peroxide (33.32%, 0.5 mmol) in *tert*-amyl alcohol was added in five portions (5×0.1 mmol) to a catalyst mixture ($FeCl_3$·6H_2O (4.17×10^{-3} M), H_2(pydic) (4.17×10^{-3} M), (*S,S*)-**4a** (0.01 M)) in the same solvent in the absence of substrate at room temperature, a new band in the UV trace developed progressively at 465 nm (Figure 1, b–f), but did not increase in intensity after addition of the last portion. The identity of this species is currently under investigation. However, it is likely to be either an LFe^{III}–OOH or an LFe^{III}–OO–Fe^{III}L complex. Homolysis or heterolysis of the O–O bond of either of these species would lead to high-valent Fe=O species that are suggested to be the actual oxidants.

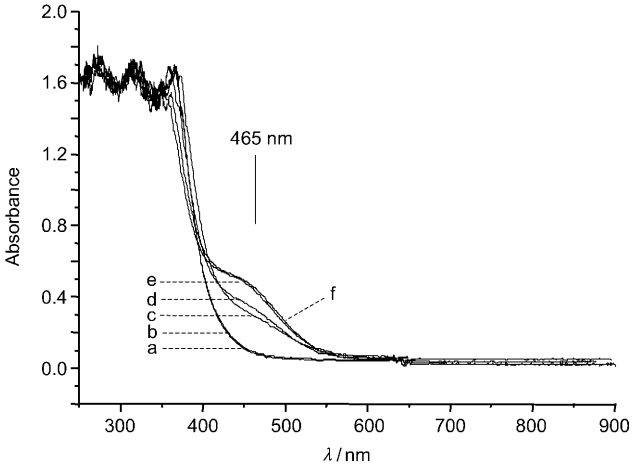

Figure 1. UV/Vis spectra of the catalyst mixture ($FeCl_3$·6H_2O (4.17×10^{-3} M), H_2(pydic) (4.17×10^{-3} M), (*S,S*)-**4a** (0.01 M)) in *tert*-amyl alcohol a) before the addition of H_2O_2 and b)–f) after the portionwise addition of a dilute solution of aqueous H_2O_2 (33.32%, 0.5 mmol; 0.1 mmol per portion) in *tert*-amyl alcohol, added at 0, 4, 7, 10, and 13 min, respectively.

The absorbance at $\lambda=465$ nm is probably due to a hydroperoxo-to-Fe^{III} charge-transfer transition and lies in the range reported for related low-spin LFe^{III}–OOH complexes.[24] On the other hand, when the catalyst mixture was treated with small portions of hydrogen peroxide in the presence of *trans*-stilbene, the band at $\lambda=465$ nm was no longer visible. Instead, a new band appeared at $\lambda=422$ nm that is likely to be due to the transformation product of the species with an absorbance at $\lambda=465$ nm after oxygen transfer (Figure 2). Raman and FTIR spectroscopic studies that were conducted alongside the UV/Vis spectroscopic measurements gave bands that corresponded to alkene and epoxide functionali-

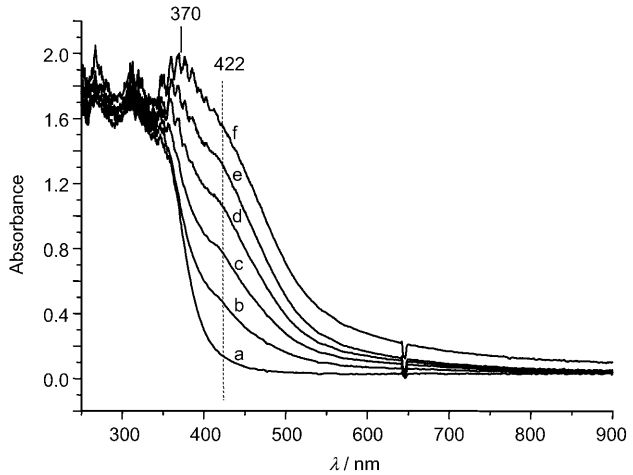

Figure 2. UV/Vis spectra of the reaction mixture ($FeCl_3$·6H_2O (0.025 mmol, 4.17×10^{-3} M), H_2(pydic) (0.025 mmol, 4.17×10^{-3} M), (*S,S*)-**4a** (0.06 mmol, 0.01 M), **1a** (0.5 mmol, 0.08 M)) in *tert*-amyl alcohol a) before the addition of H_2O_2 and b)–f) after the portionwise addition of a dilute solution of aqueous H_2O_2 (33.32%, 0.5 mmol; 0.1 mmol per portion) in *tert*-amyl alcohol.

ties. We could not observe peaks that were diagnostic of Fe–O or O–O bonds in the Raman and FTIR spectra, presumably because of the overlap of these bands with those of the alkene.

EPR spectroscopy: To determine whether paramagnetic Fe species are formed before or during the reaction and how this might change upon the sequential addition of each component, we followed the EPR spectra of each component as it was added to the reaction solution in *tert*-amyl alcohol, starting with the iron salt. $FeCl_3{\cdot}6H_2O$ (Figure 3, ——) has a sharp signal at $g=1.98$, which is comparable to the reported[34] value of $g=2.022$ for $FeCl_3{\cdot}6H_2O$ at room temperature

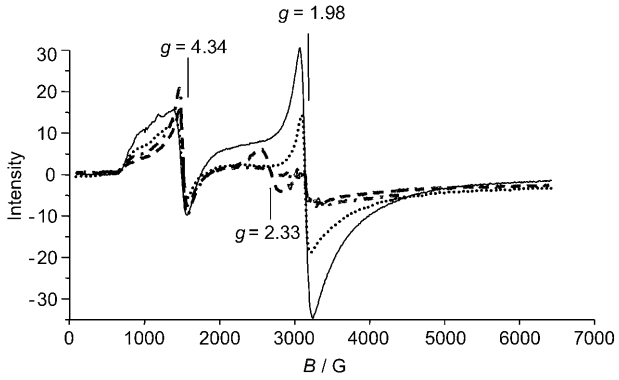

Figure 3. Graphs showing the change in the EPR signals of the reaction mixture upon the successive addition of H_2(pydic) (0.025 mmol, 0.0125 M; •••••), (*S*,*S*)-**4a** (0.06 mmol, 0.03 M; – – –), and **1a** (0.5 mmol, 0.25 M; –•–•) to a base solution of $FeCl_3{\cdot}6H_2O$ (0.025 mmol, 0.0125 M; ——) in *tert*-amyl alcohol ($T=77$ K).

and a broader signal at $g=4.34$, which is typical of a high-spin Fe^{III} species with rhombic distortion. After addition of an equal amount of H_2(pydic) (Figure 3, •••••), both signals weakened in intensity, which suggests that complex formation between Fe and H_2(pydic) had occurred. When (*S*,*S*)-**4a** (2.4 equiv with respect to Fe; Figure 3, – – –) was added, a new signal at $g=2.33$ ($g_\perp$) appeared and the original signal at $g=1.98$ almost disappeared. This suggests that formation of a low-spin chiral (pydic)Fe–(*S*,*S*)-**4a** complex in solution had occurred. Finally, when excess *trans*-stilbene (20 equiv with respect to Fe; Figure 3, –•–•) was added, only the signal at $g=4.34$ remained. While it is not clear how the alkene functionality contributes to the disappearance of the signal at $g_\perp=2.33$, we cannot rule out additional coordination to a metal center or displacement of the chiral ligand from the coordination sphere. Upon addition of only 0.1 mmol of hydrogen peroxide (33.32%, 0.2 equiv with respect to the alkene), all signals except that at $g=4.34$ almost completely disappeared (Figure 4b). This suggested that formation of a dimeric Fe^{III} species had occurred, which could not be detected due to the anti-ferromagnetic coupling of unpaired electrons. We propose that the species with a *g* value of 4.34 is not an active catalyst for the epoxidation because neither its magnitude nor its position changed much in the course of the reaction.

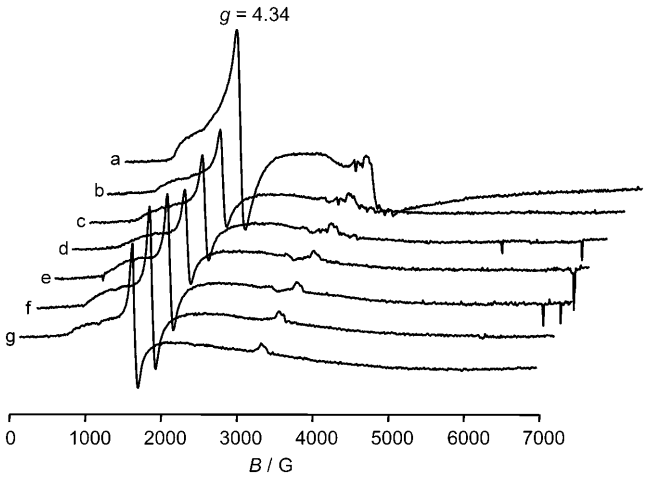

Figure 4. Graphs showing the change in the EPR signals of the reaction mixture ($FeCl_3{\cdot}6H_2O$ (0.025 mmol, 0.0125 M), H_2(pydic) (0.025 mmol, 0.0125 M), (*S*,*S*)-**4a** (0.06 mmol, 0.03 M), **1a** (0.5 mmol, 0.25 M)) in *tert*-amyl alcohol a) before the addition of H_2O_2 and b)–g) after the portionwise addition of aqueous H_2O_2 (33.32%, 91.13 μL, 1 mmol) in *tert*-amyl alcohol (total volume 1.0 mL); 5×100 μL, 0.1 mmol; $1\times=500$ μL, 0.5 mmol. All spectra were recorded at 77 K.

Spin trapping with TEMPO: A trace amount of 2,2,6,6-tetramethylpiperidine-1-oxyl (TEMPO; 1.282×10^{-4} mmol) in *tert*-amyl alcohol was added to the standard reaction mixture ($FeCl_3{\cdot}6H_2O$ (0.025 mmol), H_2(pydic) (0.025 mmol), (*S*,*S*)-**4a** (0.06 mmol), *trans*-stilbene (0.5 mmol)) in *tert*-amyl alcohol (2 mL) and the EPR spectrum was recorded at 77 K. The resulting spectrum was dominated by the signal of TEMPO (Figure 5A, ——). After an aqueous solution of hydrogen peroxide (30%, 0.5 mmol) in *tert*-amyl alcohol (0.5 mL) was added to the reaction flask and stirred for a few minutes, it took an induction period of about 30 s for the expected brown coloration to appear. When we recorded the spectrum, the TEMPO signal had disappeared completely (Figure 5A, – – –). This finding is consistent with the formation of transient carbon radicals during the reaction, which could be trapped by the radical scavenger at a very high rate (Scheme 2, left). The rate of combination of the benzyl radical with TEMPO is known to approach diffusion

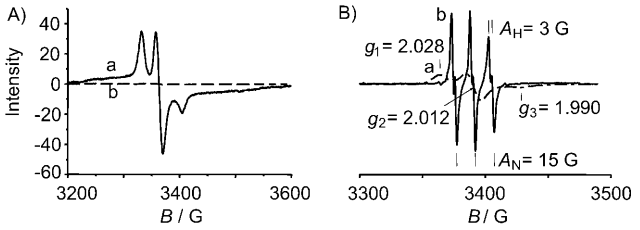

Figure 5. The results of spin trapping experiments with A) TEMPO; ——: $FeCl_3{\cdot}6H_2O$, H_2(pydic), (*S*,*S*)-**4a**, **1a**, TEMPO, $T=77$ K; – – –: after the addition of H_2O_2 (0.5 mmol) and B) BPN; –•–•: $FeCl_3{\cdot}6H_2O$, H_2(pydic), (*S*,*S*)-**4a**, **1a**, BPN, H_2O_2 (1.0 mmol), $T=77$ K; ——: $T=298$ K. See the Experimental Section for conditions.

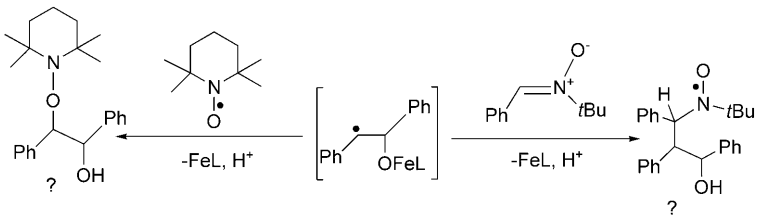

Scheme 2. Possible paths for the spin trapping of a transient carbon radical by TEMPO (left) and BPN (right).

control.[25] However, the possibility of signal disappearance due to other reactions of TEMPO, rather than the trapping of radicals, under these reaction conditions cannot be ruled out. Therefore, we repeated the experiment with a nitrone spin trap, the radical adduct of which should show distinct EPR signals.

Spin trapping with BPN: To support the argument above, the spin-trapping experiment was repeated by using *N-tert*-butylphenylnitrone (BPN; 0.5 mmol) as a radical trap, under the same reaction conditions described for TEMPO (Scheme 2, right). The EPR spectrum of this reaction mixture at room temperature revealed no signals resulting from nitroxyl radicals. Aqueous hydrogen peroxide (33.32%, 1.0 mmol) in *tert*-amyl alcohol was added in five portions and the EPR spectrum was recorded after each addition. The spectrum at 77 K was too broad for clear interpretation (Figure 5B, –•–•). At room temperature, however, the gradual development of a triplet of doublets (the hyperfine coupling constants for the nitrogen and hydrogen nuclei are $A_N = 15$ and $A_H = 3$ G, respectively) that was assignable to a radical adduct of BPN was observed (Figure 5B, ——). The signal recorded after the final addition is shown in Figure 5B. Although BPN is not specific to carbon radicals, this complementary finding suggests that, under the experimental conditions, the formation of epoxides proceeds via the formation of radical intermediates that can be trapped by appropriate radical scavengers. The spin adducts are currently being characterized.

Kinetic studies

Direct kinetic measurement of the asymmetric epoxidation of styrene with hydrogen peroxide: To obtain kinetic data for a representative asymmetric epoxidation at room temperature, the epoxidation of styrene (489.64 mM) with hydrogen peroxide (30%, 25.0 mM) in the presence of (*S,S*)-**5a** (0.6001 mM), H_2(pydic) (0.127 mM), and $FeCl_3{\cdot}6H_2O$ (0.250 mM) in *tert*-amyl alcohol was evaluated by using GC with dodecane as the internal standard. The concentration of styrene oxide against time was fitted by using first-order exponential decay with the aid of a computer to obtain [styrene oxide]$_\infty$ (Figure 6). The observed pseudo-first-order rate constant ($k_{obs} = 3.972 \times 10^{-4}\,s^{-1}$) was obtained from a plot of log([styrene oxide]$_\infty$–[styrene oxide]$_t$) versus time (Figure 7), according to Equation (1):

$$\log([\text{styrene oxide}]_\infty - [\text{styrene oxide}]_t) = -k_{obs}t + \text{constant} \quad (1)$$

with which the catalysis rate constant ($k_{cat} = 8.112 \times 10^{-4}\,M^{-1}\,s^{-1}$) was calculated from $k_{obs}/[\text{styrene}]_{init} = k_{cat}$. Each reaction was repeated three times.

To determine the relative ratios of (*S,S*)-**5a** and H_2(pydic) in the active catalyst, we plotted k_{cat} versus [(*S,S*)-**5a**]/[H_2(pydic)] (Figure 8; conditions: $[FeCl_3{\cdot}6H_2O]/[H_2(pydic)] = 1{:}1$, [Fe] = 0.25 mM, $[\text{styrene}]_{init} = 489.64$ mM, $[H_2O_2]_{init} = 30\%$, 25.0 mM). This plot shows that the slowest measured rate was at [(*S,S*)-**5a**]/[H_2(pydic)] ≈ 2.0. When [(*S,S*)-**5a**]/[H_2(pydic)] ≈ 2.5, a steady increase in reaction rate was observed until a peak was reached at [(*S,S*)-**5a**]/[H_2(pydic)] ≈ 3.5, which was followed by a slight fall at [(*S,S*)-**5a**]/[H_2(pydic)] ≈ 4.0. After this drop the rate increased again, which suggests that more than one species was involved in catalyzing this reaction.

A plot of k_{cat} versus [H_2(pydic)]/[Fe] (Figure 9; conditions: $[FeCl_3{\cdot}6H_2O]/[(S,S)\text{-}\mathbf{5a}] = 1{:}2.4$, [Fe] = 0.25 mM, $[\text{styrene}]_{init} = 489.64$ mM, $[H_2O_2]_{init} = 30\%$, 25.0 mM) shows a maximum

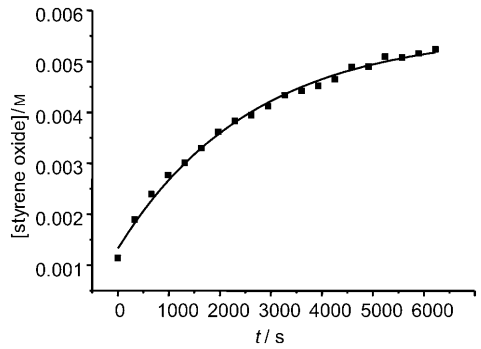

Figure 6. A typical first-order exponential decay fitting of [styrene oxide] versus time.

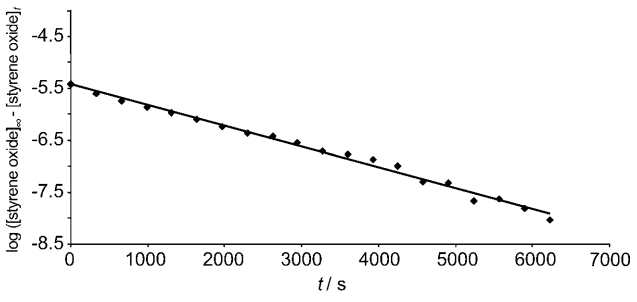

Figure 7. Plot of log([styrene oxide]$_\infty$–[styrene oxide]$_t$) versus time, which gives the pseudo-first-order rate constant as $3.972 \times 10^{-4}\,s^{-1}$ ($y = -3.972 \times 10^{-4}x + 5.4342$, $R^2 = 9.9076 \times 10^{-1}$).

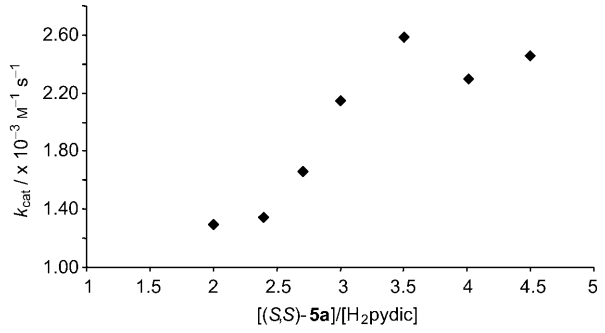

Figure 8. Plot of k_{cat} versus [(*S*,*S*)-**5a**]/[H_2(pydic)] ($FeCl_3$·6H_2O/H_2-(pydic) = 1:1 and [Fe] = 0.25 mM).

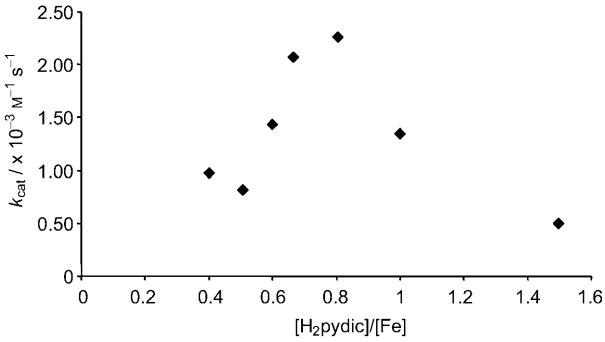

Figure 9. A plot of k_{cat} versus [H_2(pydic)]/[Fe] ($FeCl_3$·6H_2O/(*S*,*S*)-**5a** = 1:2.4 and [Fe] = 0.25 mM).

rate at [H_2(pydic)]/[Fe] ≈ 0.8. At [H_2(pydic)]/[Fe] ≈ 1.0 and above, the rate dramatically decreased, which suggested that the optimum [H_2(pydic)]/[Fe] ratio (*X*) in the active species was $0.8 \leq X \leq 1.0$. The linear dependence of k_{cat} on [$FeCl_3$·6H_2O] was established from a plot of k_{cat} versus [$FeCl_3$·6H_2O] (Figure 10).

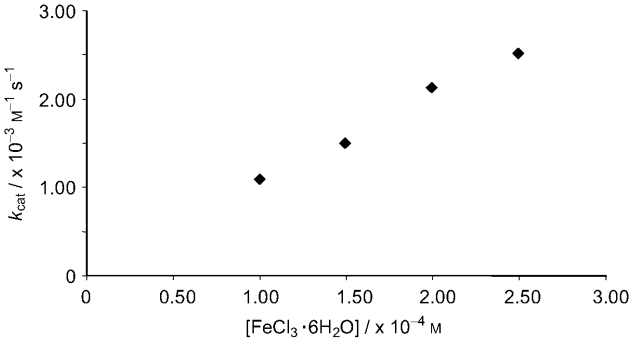

Figure 10. A plot of k_{cat} versus [$FeCl_3$·6H_2O] ($FeCl_3$·6H_2O/(*S*,*S*)-**5a**/H_2-(pydic) = 1:0.8:2.8).

Competitive asymmetric epoxidation of para-substituted styrenes with hydrogen peroxide: To assess whether the formation of a carbon radical intermediate is involved in the epoxidation of aromatic alkenes with hydrogen peroxide in the presence of $FeCl_3$·6H_2O/(*S*,*S*)-**5a**/H_2(pydic), the competitive asymmetric epoxidation of various *para*-substituted styrenes (Table 4) was examined more closely. In this case, the

Table 4. Relative rate constants for the competitive epoxidation of *para*-substituted styrenes with hydrogen peroxide and σ values for the corresponding substituents.

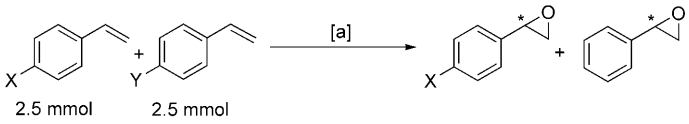

Entry	X	k_{rel}	logk_{rel}	σ_{JJ}·[b]	σ_{mb}[b]
1	H	1.00	0	0	0
2	Me	2.52	0.925	0.15	−0.29
3	F	1.56	0.443	−0.02	−0.24
4	Cl	1.22	0.201	0.22	0.11
5	CF_3	0.34	−1.077	−0.01	0.49

[a] Conditions: $FeCl_3$·**6**H_2O (5 mol%), H_2(pydic) (5 mol%), (*S*,*S*)-**5a** (12 mol%), H_2O_2 (30%, 0.5 mmol), *tert*-amyl alcohol, RT. [b] See ref. [26]

energy of the transition state (TS) was expected to be affected by polar and spin-delocalization effects. These effects can be quantified separately by employing the dual-parameter Hammett correlation [Eq. (2)] developed by Jiang and Ji.[26]

$$\log k_{rel} = \rho_{JJ}\cdot\sigma_{JJ}\cdot + \rho_{mb}\sigma_{mb} \quad (2)$$

A straight line with a slope of 1.00 ($R^2 = 0.999$) was obtained from a plot of logk_{rel} versus $2.07\sigma_{JJ}\cdot - 2.13\sigma_{mb}$ (Figure 11). This linear free-energy correlation with polar

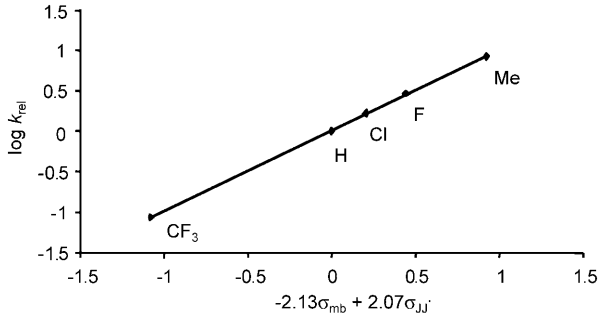

Figure 11. Dual-parameter Hammett correlation for the epoxidation of styrene and *para*-substituted styrenes, according to Table 4. $y = 1.0025x$, $R^2 = 0.9994$, $|\rho_{mb}/\rho_{JJ}\cdot| = 1.03$.

and spin-delocalization effects suggested the formation of a benzylic radical species in the TS of the arylalkene epoxidation. The large positive $\rho_{JJ}\cdot$ value of 2.07 suggests that the reaction is promoted by spin delocalization at the radical center, whereas the negative ρ_{mb} value of −2.13 is consistent with the electrophilic nature of the active oxidant. However, the magnitude of $|\rho_{mb}/\rho_{JJ}\cdot|$, 1.03, suggests that polar substituent effects are slightly more important than spin-delocalization effects.[26]

Competitive asymmetric epoxidation of deuterated styrenes with hydrogen peroxide: For the determination of the secondary kinetic isotope effect (KIE), the competitive epoxidations of styrene and deuterated styrenes (α-[D]styrene and β-[D_2]styrene) were conducted under the conditions shown in Schemes 3 and 4.

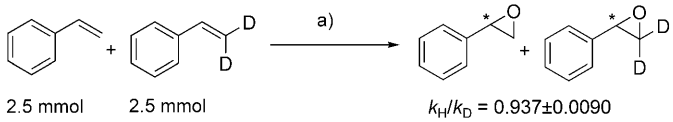

Scheme 3. The competitive epoxidation of styrene and β-[D_2]styrene. a) $FeCl_3$·6H_2O (5 mol%), H_2(pydic) (5 mol%), (*S*,*S*)-**5a** (12 mol%), H_2O_2 (30%, 57 μL, 0.5 mmol), *tert*-amyl alcohol, RT.

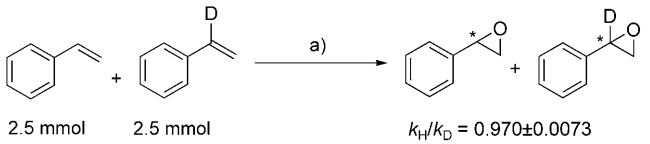

Scheme 4. The competitive epoxidation of styrene and α-[D]styrene. a) $FeCl_3$·6H_2O (5 mol%), H_2(pydic) (5 mol%), (*S*,*S*)-**5a** (12 mol%), H_2O_2 (30%, 0.5 mmol), *tert*-amyl alcohol, RT.

The observation of a significant inverse secondary KIE in the case of β-[D_2]styrene ($k_H/k_D = 0.937 \pm 0.0090$) and only a small KIE ($k_H/k_D = 0.970 \pm 0.0073$) in the case of α-[D]styrene is consistent with an unsymmetrical TS in which the C–O bond formation (i.e., sp^3 hybridization) is more advanced at the β-carbon than at the α-carbon, which implies a stepwise mechanism. Assuming a high-valent Fe=O intermediate as the active oxidizing species, this finding again suggests that epoxidation under this system may involve the formation of benzylic radicals in the rate-determining step.

Nonlinear effect (NLE) studies: Since its discovery in the 1980s, the NLE has been successfully applied as a mechanistic tool in the interpretation of many catalytic asymmetric reactions.[27] The asymmetric epoxidation of *trans*-stilbene was performed with mixtures of (*S*,*S*)-**5a** and (*R*,*R*)-**5a** with varying *ee* values. A plot of the *ee* of **2a** versus the *ee* of **5a** revealed a small but clearly positive NLE (Figure 12). Following Kagan's ML_2 and reservoir models,[27] the source of the +NLE may be the formation of a less-reactive meso dimer. This indirectly suggests the existence of complex equilibria that involve several chiral Fe complexes. The relative concentrations and reactivities of these species determine the observed enantioselectivity of the reaction.

^{18}O isotope dilution studies: When the asymmetric epoxidation of *trans*-stilbene was conducted under standard conditions in the presence of a large excess of $H_2{}^{18}O$ (250 mmol, 500 equiv), no reaction took place. However, with a smaller excess of $H_2{}^{18}O$ (10 mmol), the reaction takes places

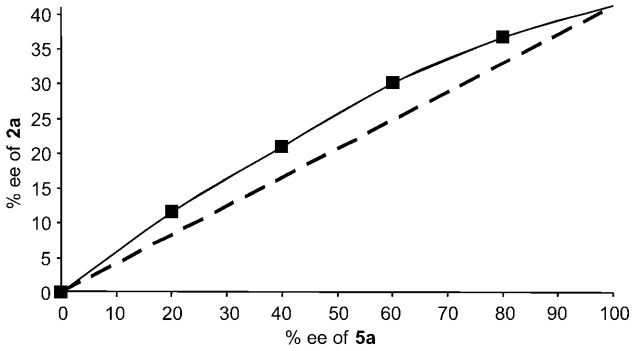

Figure 12. Graph of the *ee* of **2a** versus the *ee* of **5a**, which shows a positive NLE. – – –: Theoretical curve, ■: measured data points.

smoothly to give a quantitative yield of the unlabeled epoxide (Scheme 5) in which no trace of ^{18}O-labeled **2a** was detected. A trace amount of benzaldehyde was observed in

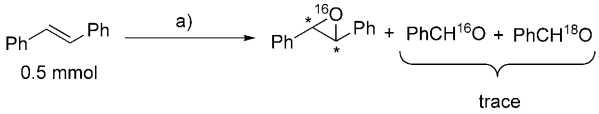

Scheme 5. Reaction scheme for the isotope dilution studies. a) $FeCl_3$·6H_2O (5 mol%), H_2(pydic) (5 mol%), (*S*,*S*)-**5a** (12 mol%), H_2O_2 (50%, 1.19 mmol), $H_2{}^{18}O$ (10 mmol), *tert*-amyl alcohol, RT.

which the label was partly found ($^{16}O/^{18}O = 88:22$). These results suggest that formation of benzaldehyde might take place in a consecutive reaction that starts from an intermediate of the catalytic cycle. In addition, the results suggest that either no high-valent Fe=O species are involved as the active oxidant or, more likely, that the rate of ^{18}O exchange with water is too low compared with the rate of ^{18}O transfer to the organic substrate at this concentration.

The number and nature of the active oxidant(s) is currently under investigation. However, based on the above observations and the wealth of accumulated literature that implicates high-valent Fe=O species as the actual active oxygen transfer agents in biological mono-oxygenations in both heme and non-heme iron enzymes and model systems,[28a–g] it is reasonable to assume that the formation of reactive high-valent Fe species, such as [(pydic)(L*)$_n$Fe=O] ($n = 1$–2), has occurred.

Assuming further that a top-on approach of the alkene to such a species is preferred over the alternative and more popular side-on approach, the following mechanistic pathway is tentatively proposed to explain the enantioselectivities. Accordingly, the Fe=O species generated by using non-benzylated ligands (*S*,*S*)-**4a–c** and their *N*-benzylated counterparts (*R*,*R*)-**5a–d** would be preferentially approached from the *Re*,*Re* face (Scheme 6, bottom), whereas the species generated by using the corresponding enantiomers of these ligands is approached from the *Si*,*Si* face (Scheme 6, top) of the *trans*-aryl alkene. The resulting L*Fe–O–aryl

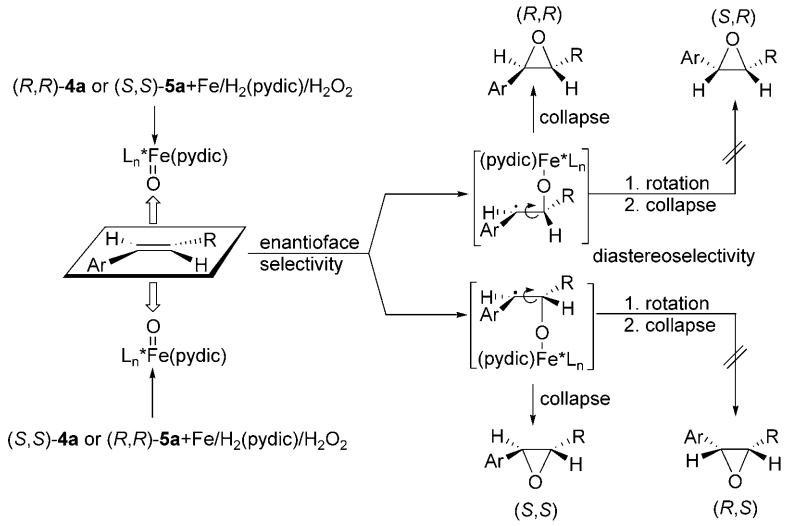

Scheme 6. Proposed mechanistic pathways to explain the enantioselectivity of this reaction.

radical species would collapse by a rebound mechanism to give the experimentally observed optically active (*S*,*S*)- and (*R*,*R*)-epoxides, respectively. The alternative pathway, in which rotation precedes collapse, is unlikely because we did not observe the corresponding diastereomeric *cis*-epoxides. Therefore, enantioselectivity is determined by the efficiency of the first step. While this mechanism seems plausible, steric factors on the substrate can dramatically alter both the reaction rate and face selectivity, as previously observed.[17]

Conclusion

The Fe-catalyzed asymmetric epoxidation of aromatic alkenes with hydrogen peroxide as the oxygen source and a chiral Fe catalyst generated from $FeCl_3{\cdot}6H_2O$, H_2(pydic), and the novel, readily accessible, chiral (*S*,*S*)-**5a** has been extended to sterically less demanding alkenes. The asymmetric epoxidation of styrenes gives almost complete conversions, but lower *ee* values compared with larger alkenes. (*S*,*S*)-**5a** and (*S*,*S*)-**4a** (the non-benzylated precursor of (*S*,*S*)-**5a**) give opposite enantiomers of *trans*-stilbene oxide ((*R*,*R*)-**2a** and (*S*,*S*)-**2a**, respectively). *cis*-Alkenes are generally poorer substrates than *trans*-alkenes for the current asymmetric epoxidation, and steric factors are more important than electronic factors in controlling the enantioselectivity. Mass spectrum signals corresponding to Fe complexes, such as $[FeCl(L^*)_2(pydic)]{\cdot}HCl$ in which $L^* = (S,S)$-**4a** or (*S*,*S*)-**5a**, were identified by ESIMS studies of the catalyst mixture. Hydrogen peroxide may react with this species to initially form $[Fe^{III}(L^*)_2(OOH)(pydic)]$. Homolysis or heterolysis of the O–O bond of such a species would generate $Fe^{IV}{=}O{+}{\cdot}OH$ radicals and $Fe^{V}{=}O{+}{}^{-}OH$, respectively. The high-valent Fe=O species are more likely oxidants than η_2-$LFe^{III}O_2H$ and ·OH radicals. We have ruled out the possibility that ·OH radicals play any significant role in the current alkene epoxidation because of the unusually high yields and *ee* values of the epoxides. A UV/Vis study of the catalyst mixture with (*S*,*S*)-**4a** as the chiral ligand revealed a species that had an absorbance peak at $\lambda =$ 465 nm upon the addition of hydrogen peroxide, which is currently being characterized. The epoxidation reaction appears to proceed via radical intermediates that could be intercepted by using radical scavengers. An inverse secondary isotope effect (KIE) of $k_H/k_D = 0.93$ for the β-carbon and $k_H/k_D = 0.97$ for the α-carbon of styrene suggests an unsymmetrical TS in which oxygen transfer is nonconcerted. The epoxidation of *para*-substituted styrenes revealed a linear dual-parameter Hammett plot with a slope of 1.00, which suggests that the formation of a benzylic radical species in the TS had occurred. Epoxidation of *trans*-stilbene in the presence of excess $H_2{}^{18}O$ resulted in an absence of the label in the epoxide product, which is probably due to a much slower rate of label exchange compared with O transfer from a high-valent Fe=O species. The reaction showed a small but significant NLE, which suggested the participation of several chiral Fe complexes in catalyzing the reaction, the relative concentrations and reactivities of which determine the observed *ee* value. Efforts to identify these species and study the mechanism in greater detail are under way. Although much remains to be done in terms of improving *ee* values and increasing substrate scope, the achievement of a significant asymmetric alkene epoxidation with simple iron salts and hydrogen peroxide at room temperature serves as a useful biomimetic functional model for non-heme iron alkene mono-oxygenases[28h–i] and helps stimulate further research in this field.

Experimental Section

General: A Leco CHNS-932 analyzer was used for elemental analyses. An AMD 402/3 mass spectrometer was used for recording mass spectra. High-resolution mass spectrometry experiments were performed by using an Agilent Series 1200 HPLC system and an Agilent 1969A time-of-flight mass spectrometer. The TOF-MS conditions (positive-ion mode) with a dual sprayer API-ES source were as follows: nebulizer and drying gas, nitrogen; nebulizer pressure = 241.313 kPa, drying gas flow = 12 L min^{-1}, drying gas temperature = 300 °C, capillary voltage = 4 kV, fragmentor voltage = 225 V, skimmer voltage = 60 V, octopole voltage = 250 V, and mass reference (*m*/*z*): 121.050873 and 922.009798. The mobile phase consisted of 10% H_2O (0.1% HCOOH) and 90% MeOH at a flow rate of 0.5 mL min^{-1}. GC analysis was performed by using a Hewlett Packard HP 6890 gas chromatograph with a flame ionization detector (FID). UV/

Vis spectroscopy measurements were carried out by using an Avantes fiber-optic spectrometer (AVASPEC) with a fiber-optic sensor in transmission against the solvent (*tert*-amyl alcohol or acetonitrile) as the reference. FTIR spectroscopy measurements were conducted by using a fiber-optic Diamant-ATR probe, coupled with an FTIR-spectrometer (Nicolet Avatar 370). Raman spectroscopy measurements were carried out by using a fiber-optical RXN spectrometer (Kaiser Optical Systems, laser $\lambda = 785$ nm) with the laser power set at 100 mW. UV/Vis, FTIR and Raman spectroscopic data were collected simultaneously. EPR investigations were conducted separately with a Bruker CW-EPR spectrometer ELEXSYS 500-10/12 in X-Band with the following settings: microwave frequency = 9.5 GHz, power = 6.3 mW, modulation frequency = 100 kHz, and amplitude = 0.5 mT. Alkenes **1a**, **1d**, and **1l–s**; ligands (*S*,*S*)-**3**, (*S*,*S*)-**4a**, and (*R*,*R*)-**4a**; pyridine-2,6-dicarboxylic acid; $FeCl_3{\cdot}6H_2O$; hydrogen peroxide;[32] the aldehydes and arenesulfonyl chlorides used for the synthesis of the ligands; the spin traps and the dry solvents are commercial products (Sigma-Aldrich, Fluka, Merck) and were used as received. Alkenes **1b**, **1c**, and **1e–i** were synthesized by a McMurry[29] coupling of the corresponding alkyl-substituted benzaldehydes and obtained in high yields and purities. Alkenes **1j** and **1v** were synthesized by the Heck reaction of 4-*tert*-butylbromobenzene with 2-vinylnaphthalene or styrene, respectively, by modifying the method of Chandrasekhar et al.[30] Alkenes **1k** and **1t** were synthesized by protecting *trans*-cinnamyl alcohol with triphenylsilyl chloride or *tert*-butyldimethyl silylchloride, respectively, in the presence of pyridine. All racemic epoxides **2**, which were necessary references for the chiral HPLC data, were synthesized by epoxidation with metachloroperbenzoic acid (MCPBA). Typically, one to two equivalents of a solution of MCPBA in dichloromethane (CH_2Cl_2) were added dropwise to an ice-cooled solution of the alkene in CH_2Cl_2. After stirring overnight at RT, the solvent was removed under reduced pressure and the residue was purified by flash chromatography to give high yields of the corresponding epoxides (see the Supporting Information for analytical data).

General procedure for the synthesis of (*S*,*S*)-4b–g:[31] A solution of the corresponding arene sulfonyl chloride (4.86 mmol, 1.0 equiv) in CH_2Cl_2 (5 mL) was added dropwise with stirring to a solution of diamine (*S*,*S*)-**3** (1.032 mg, 4.86 mmol) and diisopropylethyl amine (DIPEA, 0.923 mL) in CH_2Cl_2 (10 mL) at 0 °C over 30 min. Then the mixture was stirred at RT for 5 h. The progress of the reaction was monitored by TLC. After complete conversion, water (5 mL) was added and the phases separated. The aqueous phase was then extracted twice with CH_2Cl_2 (5 mL). The combined organic phases were dried, concentrated, and purified by silica gel chromatography and characterized (see the Supporting Information).

Synthesis of (*R*,*R*)-5a, (*S*,*S*)-5b–i: These ligands were synthesized by treating the corresponding *N*-amino-*N*′-arenesulfonyl diphenyl ethylene diamine ligands and benzaldehyde ((*R*,*R*)-**5a**, (*S*,*S*)-**5b–g**), or 4-methylbenzaldehyde ((*S*,*S*)-**5i**), according the reductive alkylation procedure given for the synthesis of (*S*,*S*)-**5a**[17a] (see the Supporting Information for analytical data).

General procedure for the Fe-catalyzed asymmetric epoxidation of alkenes 1a–y: Pyridine-2,6-dicarboxylic acid (4.24 mg, 0.025 mmol), ferric chloride hexahydrate (6.76 mg, 0.025 mmol), ligands (*S*,*S*)-**3**, (*S*,*S*)-**4a–g**, or (*S*,*S*)-**5a–i** (0.06 mmol), and alkenes **1a–y** (0.5 mmol) were mixed in *tert*-amyl alcohol (9 mL) and stirred at RT for about 30 min. The resulting mixture usually assumed a pale yellow color. For the GC determination of yields and conversions, dodecane (100 μL) was added as the internal standard. After taking samples for GC analysis, aqueous hydrogen peroxide ("30%", 1 mmol) in *tert*-amyl alcohol (1 mL) was added to this mixture over one hour by using a syringe pump. [A generally accurate volume of the "30%" solution can not be given in this case because the peroxide content (and thus the density) of this material varies considerably with time. Therefore, before each experiment we determined the peroxide content (%) by titration. For multiple runs we weighed the amount corresponding to 10 mmol H_2O_2 into a 10 mL volumetric flask, filled with the solvent to volume and withdrew the required amount (1 mL, 1 mmol) of the solution using by a syringe (see also ref. [32]). For single runs 1 mmol H_2O_2 may also be directly diluted with solvent to 1 mL before introduction into the reaction flask.] In most cases, complete conversion was achieved after this time (determined by GC and/or TLC monitoring). For preparative purposes, excess peroxide was eliminated by adding a saturated aqueous solution of sodium sulfite (1 mL) and shaking well. After addition of diethyl ether (10 mL), the phases were separated, and the aqueous phase was extracted with diethyl ether (3 × 10 mL). The combined organic phases were then dried over anhydrous $MgSO_4$. After filtration and solvent removal by rotary evaporator, the crude product was either directly analyzed by chiral HPLC to determine its *ee* or purified by silica gel chromatography on a short column (eluent: hexane/ethyl acetate 20:1, 1% Et_3N) for full characterization.

General procedure for catalyst NLE studies of asymmetric epoxidation with hydrogen peroxide: Compound (*R*,*R*)-**5a** (24.66 mg, 0.054 mmol), (*S*,*S*)-**5a** (2.74 mg, 0.006 mmol), H_2(pydic) (4.17 mg, 0.025 mmol), $FeCl_3{\cdot}6H_2O$ (6.76 mg, 0.025 mmol), and *trans*-stilbene (90.1 mg, 0.500 mmol) were heated in *tert*-amyl alcohol (9.0 mL) in a 25 mL Schlenk tube until a clear yellow solution formed (≈1 min). After the reaction mixture had cooled to RT, dodecane (GC internal standard, 100 μL) was added. Aqueous hydrogen peroxide (30%, 113 μL, 1.0 mmol) in *tert*-amyl alcohol (887 μL) was added to this reaction mixture over a period of 1 h by using a syringe pump. After this addition, aliquots were taken from the reaction mixture and subjected to GC analysis for the determination of yield and conversion data. The reaction mixture was then quenched with an aqueous solution of Na_2SO_3 (≈10 mL), extracted with dichloromethane (2 × 10 mL), and washed with water (≈20 mL). The combined organic layers were dried over $MgSO_4$ and evaporated under reduced pressure to give the crude epoxides, which were then dissolved in *n*-hexane for HPLC measurement.

General procedure for the competitive asymmetric epoxidation of *para*-substituted styrene with hydrogen peroxide: Compound (*S*,*S*)-**5a** (27.42 mg, 0.060 mmol), H_2(pydic) (4.17 mg, 0.025 mmol), and $FeCl_3{\cdot}6H_2O$ (6.78 mg, 0.025 mmol) were heated in *tert*-amyl alcohol (9.0 mL) in a 25 mL Schlenk tube until a clear yellow solution formed (≈1 min). After the reaction mixture had cooled to RT, styrene (2.5 mmol), *p*-methylstyrene (2.5 mmol), and dodecane (GC internal standard, 100 μL) were added. Aqueous hydrogen peroxide (30%, 57 μL, 0.5 mmol) in *tert*-amyl alcohol (276 μL) was added to this reaction mixture over a period of 1 h by using a syringe pump. After the addition, aliquots were taken from the reaction mixture and subjected to GC analysis for the determination of yield and conversion data.

General procedure for the competitive asymmetric epoxidation of deuterated styrenes with hydrogen peroxide

For styrene and β-*[D$_2$]styrene*: Compound (*S*,*S*)-**5a** (27.42 mg, 0.060 mmol), H_2(pydic) (4.17 mg, 0.025 mmol), and $FeCl_3{\cdot}6H_2O$ (6.78 mg, 0.025 mmol) were heated in *tert*-amyl alcohol (9.0 mL) in a 25 mL Schlenk tube until a clear yellow solution formed (≈1 min). After the reaction mixture had cooled to RT, styrene (2.5 mmol), β-[D_2]styrene (2.5 mmol), and dodecane (GC internal standard, 100 μL) were added. To this reaction mixture, aqueous hydrogen peroxide (30%, 57 μL, 0.5 mmol) in *tert*-amyl alcohol (276 μL) was added over a period of 1 h by using a syringe pump. After the addition, aliquots were taken from the reaction mixture and subjected to GC analysis for the determination of yield and conversion data. The reaction mixture was then quenched with an aqueous solution of Na_2SO_3 (≈10 mL), extracted with dichloromethane (2 × 10 mL), and washed with water (≈20 mL). The combined organic layers were dried over $MgSO_4$ and evaporated under reduced pressure to give the crude epoxides, which were then purified by silica gel chromatography (70–230 mesh, neutralized with 1% Et_3N) with hexane to hexane/ethyl acetate (100:3) as the gradient eluent. The selectivity was determined by ^{1}H NMR spectroscopy. Each reaction was repeated three times.

For styrene and α-*[D]styrene*: The procedure was the same as described above, except that α-[D]styrene (2.5 mmol) was used instead of β-[D_2]styrene.

General procedure for asymmetric epoxidation with hydrogen peroxide in the presence of $H_2^{18}O$: Compound (*S*,*S*)-**5a** (27.42 mg, 0.060 mmol), H_2(pydic) (4.17 mg, 0.025 mmol), $FeCl_3{\cdot}6H_2O$ (6.78 mg, 0.025 mmol), and *trans*-stilbene (90.1 mg, 0.500 mmol) were heated in *tert*-amyl alcohol (9.0 mL) in a 25 mL Schlenk tube until a clear yellow solution formed

(≈1 min). After the reaction mixture had cooled to RT, $H_2{}^{18}O$ (180 μL, 10.0 mmol) and dodecane (GC internal standard, 100 μL) were added. To this reaction mixture, an aqueous solution of hydrogen peroxide (50%, 68 μL, 1.19 mmol) in *tert*-amyl alcohol (932 μL) was added over a period of 1 h by using a syringe pump. After this addition, aliquots were taken from the reaction mixture and subjected to GC-FID analysis for determination of yield and conversion data. The reaction mixture was then further analyzed by GC-MS.

General procedure for the direct kinetic measurement of the asymmetric epoxidation of styrene with hydrogen peroxide: Compound (*S*,*S*)-**5a** (27.40 mg, 0.060 mmol), H_2(pydic) (2.12 mg, 0.013 mmol), and $FeCl_3{\cdot}6H_2O$ (6.75 mg, 0.025 mmol) were heated in *tert*-amyl alcohol (10 mL) in a 50.00 mL volumetric flask until a clear yellow solution formed (≈1 min.). After the reaction mixture had cooled to RT, the catalyst solution was diluted up to the 50.00 mL mark with *tert*-amyl alcohol. Dodecane (GC internal standard, 100 μL, 73.77 mg, 0.433 mmol), styrene (573 μL, 509.96 mg, 4.896 mmol), and the catalyst solution (5.00 mL) were added to a 10.00 mL volumetric flask. It was then diluted up to the 10.00 mL mark with *tert*-amyl alcohol. Aqueous hydrogen peroxide (30%, 29.0 μL, 0.250 mmol) was added at once and the reaction mixture was vigorously shaken. This solution was transferred to a GC vial for GC-FID analysis, and the styrene oxide concentration was determined at approximately 4.5 min intervals at RT ((23.9 ± 0.99) °C). The concentration of styrene oxide versus time was then fitted with first-order exponential decay by using the software Origin 7.5 SR5 [v 7.5870 (B870)][33] to obtain $[\text{styrene oxide}]_\infty$. The observed rate constant was obtained by plotting $\log([\text{styrene oxide}]_\infty - [\text{styrene oxide}]_t)$ versus time (see [Eq. (1)] and $k_{obs}[\text{styrene}]_{init} = k_{cat}$). Each reaction was repeated three times.

General procedure for the simultaneous UV/Vis, Raman, and IR spectroscopic investigation of the catalyst mixture in the absence of 1a: $FeCl_3{\cdot}6H_2O$ (6.76 mg, 0.025 mmol), H_2(pydic) (4.24 mg, 0.025 mmol), and (*S*,*S*)-**4a** (22.01 mg, 0.06 mmol) in *tert*-amyl alcohol (6 mL) were added to a 10 mL glass beaker. The UV/Vis, Raman, and IR spectroscopic data were recorded simultaneously by passing UV light through a quartz cuvette mounted in the solution and by inserting an IR sensor into the solvent bulk. Then aqueous H_2O_2 (33.32%, 45.6 μmL, 0.5 mmol) in *tert*-amyl alcohol (total volume 0.5 mL) was added in five portions (5× 100 μL, 0.1 mmol) in intervals of 2 to 3 min. After each addition, the mixture was stirred well with a magnetic stir bar and the spectra were recorded (Figure 1).

General procedure for the simultaneous UV/Vis, Raman and IR spectroscopic investigation of the catalyst mixture in the presence of 1a: $FeCl_3{\cdot}6H_2O$ (6.76 mg, 0.025 mmol), H_2(pydic) (4.24 mg, 0.025 mmol), (*S*,*S*)-**4a** (22.01 mg, 0.06 mmol), and **1a** (90.15 mg, 0.5 mmol) in *tert*-amyl alcohol (6 mL) were added to a 10 mL glass beaker. The UV/Vis, Raman, and IR data were recorded were simultaneously by passing UV-light through a quartz cuvette mounted in the solution and by inserting an IR sensor into the solvent bulk. Then aqueous H_2O_2 (33.32%, 91.13 μL, 1.0 mmol) in *tert*-amyl alcohol (total volume 1 mL) was added in ten portions (10 × 100 μL, 0.1 mmol) in intervals of approximately 2 min. After each addition, the mixture was stirred well with a magnetic stir bar and the spectra were recorded. Results from the first five portions are shown in Figure 2. No significant changes occurred upon the addition of portions six to ten, and the corresponding curves are omitted for clarity.

Procedure for the EPR spectroscopic investigation of the reaction mixture in *tert*-amyl alcohol: *tert*-Amyl alcohol (2 mL) was added to a Schlenk flask and the EPR spectrum was recorded. Then $FeCl_3{\cdot}6H_2O$ (6.76 mg, 0.025 mmol), H_2(pydic) (4.24 mg, 0.025 mmol), (*S*,*S*)-**4a** (22.01 mg, 0.06 mmol), and *trans*-stilbene (90.15 mg, 0.5 mmol) were added sequentially with stirring, to make sure that every component had been fully dissolved. Slight heating and cooling to RT was necessary. The EPR spectra were recorded at RT and at 77 K, and the sample was returned to the reaction mixture after every measurement. Figure 3 shows spectra recorded at $T = 77$ K. Then aqueous H_2O_2 (33.32%, 91.13 μL, 1.0 mmol) in *tert*-amyl alcohol (total volume 1 mL) was added in 6 portions (5× = 100 μL, 0.1 mmol each, then 1 × 500 μL, 0.5 mmol) at intervals of 2 min. After each addition, the mixture was stirred well and the spectra were recorded (Figure 4).

General procedure for spin trapping with BPN: $FeCl_3{\cdot}6H_2O$ (6.76 mg, 0.025 mmol), H_2(pydic) (4.24 mg, 0.025 mmol), (*S*,*S*)-**4a** (22.01 mg, 0.06 mmol), and *trans*-stilbene (90.15 mg, 0.5 mmol) were added to a Schlenk flask and dissolved in *tert*-amyl alcohol (2 mL) by heating to about 60–70 °C for 10 min with stirring. A sample was taken and the EPR spectrum of this solution was recorded at 77 K and at RT. The sample was then returned to the reaction vessel. BPN (88.5 mg, 0.5 mmol) was added to the reaction mixture and the EPR spectrum was recorded again. No signal resulting from nitroxyl radicals was observed. The EPR sample was then returned to the reaction flask. Aqueous H_2O_2 (30%, 103.1 μL, 1.0 mmol) in *tert*-amyl alcohol (total volume 1 mL) was added in five portions (3 × 100 μL, 0.1 mmol; 1 × 200 μL, 0.2 mmol; 1 × 500 μL, 0.5 mmol) with stirring for a few minutes after each addition before the EPR spectra were recorded. Figure 5B shows the spectra recorded at 77 K and RT after the last addition.

General procedure for spin trapping with TEMPO: $FeCl_3{\cdot}6H_2O$ (6.76 mg, 0.025 mmol), H_2(pydic) (4.24 mg, 0.025 mmol), (*S*,*S*)-**4a** (22.01 mg, 0.06 mmol), and *trans*-stilbene (90.15 mg, 0.5 mmol) were added to a Schlenk tube and dissolved in *tert*-amyl alcohol (2 mL) by heating to about 60–70 °C for 10 min with stirring. A sample was taken and the EPR spectrum of this solution was recorded at 77 K and at RT. The sample was returned to the reaction mixture. A solution of TEMPO (0.2 mL, 6.41×10^{-4} M, 1.282×10^{-4} mmol) in *tert*-amyl alcohol (prepared by dissolving TEMPO (1 mg) in *tert*-amyl alcohol (10 mL)) was added to the reaction mixture. A sample was then taken and the EPR spectrum, which was dominated by the signal from TEMPO, was recorded. The sample was returned to the reaction flask. An aqueous solution of H_2O_2 (30%, 52 μL, 0.5 mmol) in *tert*-amyl alcohol (0.5 mL) was added to the reaction flask immediately and stirred for a few minutes. After an induction period of around 30 s the solution turned brown, as expected. A sample was then taken and the spectrum was recorded at 77 K. The TEMPO signal disappeared completely from the spectrum (Figure 5A).

Acknowledgements

The authors thank the Deutsche Forschungsgemeinschaft, the State of Mecklenburg-Western Pomerania, and the Federal Ministry of Education and Research (BMBF) for financial support and the analytical staff at LIKAT, lead by Dr. C. Fischer, for recording spectra and chromatograms. Dr. D. Goerdes and E. Schmidt at CELISCA are acknowledged for their assistance in measuring the ESI MS spectra.

[1] a) K. A. Jørgensen in *Transition Metals for Organic Synthesis* (Eds.: M. Beller, C. Bolm), Wiley-VCH, Weinheim, **1998**, Vol. 2, p. 157; b) K. Furuhashi in *Chirality in Industry* (Eds.: A. N. Collins, G. N. Sheldrake, J. Crosby), John Wiley, Chichester, **1992**, p. 167; c) U. Sundermeier, C. Döbler, M. Beller in *Modern Oxidation Methods* (Ed.: J. E. Bäckvall), Wiley-VCH, Weinheim, **2004**, p. 1.

[2] a) M. Tokunaga, J. F. Larrow, F. Kakiuchi, E. N. Jacobsen, *Science* **1997**, *277*, 936–938; b) A. Gayet, S. Bertilsson, P. G. Anderson, *Org. Lett.* **2002**, *4*, 3777–3779.

[3] For reviews on the asymmetric epoxidation of allylic alcohols, see: a) T. Katsuki in *Comprehensive Asymmetric Catalysis, Vol. 2* (Eds.: E. N. Jacobsen, A. Pfaltz, H. Yamamoto), Springer, Berlin, **1999**, pp. 621–648; b) R. A. Johnson, K. B. Sharpless in *Catalytic Asymmetric Synthesis* (Ed.: I. Ojima), Wiley-VCH, New York, **1993**, pp. 103–158.

[4] For reviews, see: a) E. N. Jacobsen, M. H. Wu in *Comprehensive Asymmetric Catalysis, Vol. II* (Eds.: E. N. Jacobsen, A. Pfaltz, H. Yamamoto), Springer, Berlin, **1999**, pp. 649–677; b) T. Katsuki in *Comprehensive Coordination Chemistry II, Vol. 9* (Eds.: J. A. McCleverty, T. J. Meyer), Elsevier Science, Oxford, **2003**, pp. 207–264.

[5] Y. Shi, *Acc. Chem. Res.* **2004**, *37*, 488–496.

[6] a) For a recent review, see: D. R. Kelly, S. M. Roberts, *Biopolymers* **2006**, *84*, 74–89; b) For related peptide-catalyzed asymmetric epoxidations, see: B. List, D. Kampen, *Synfacts* **2007**, 0983.
[7] For recent reviews, see: a) F. G. Gelalcha, *Chem. Rev.* **2007**, *107*, 3338–3361; b) S. Jaroch, H. Weinmann, K. Zeitler, *ChemMedChem* **2007**, *2*, 1261–1264; c) A. Berkessel, *Pure Appl. Chem.* **2005**, *77*, 1277–1284.
[8] I. W. C. E. Arends, *Angew. Chem.* **2006**, *118*, 6398–6400; *Angew. Chem. Int. Ed.* **2006**, *45*, 6250–6252.
[9] Y. Sawada, K. Matsumoto, S. Kondo, H. Watanabe, T. Ozawa, K. Suzuki, B. Saito, T. Katsuki, *Angew. Chem.* **2006**, *118*, 3558–3560; *Angew. Chem. Int. Ed.* **2006**, *45*, 3478–3480.
[10] M. Colladon, A. Scarso, P. Sgarbossa, R. A. Michelin, G. Strukul, *J. Am. Chem. Soc.* **2006**, *128*, 14006–14007.
[11] M. K. Tse, C. Döbler, S. Bhor, M. Klawonn, W. Mägerlein, H. Hugl, M. Beller, *Angew. Chem.* **2004**, *116*, 5367–5372; *Angew. Chem. Int. Ed.* **2004**, *43*, 5255–5260.
[12] For an excellent review on the current status of Fe-catalyzed organic reactions, see: C. Bolm, J. Legros, J. Le Paih, L. Zani, *Chem. Rev.* **2004**, *104*, 6217–6254.
[13] E. Rose, Q.-Z. Ren, B. Andrioletti, *Chem. Eur. J.* **2004**, *10*, 224–230.
[14] Q. F. Cheng, X. Y. Xu, W. X. Ma, S. J. Yang, T. P. You, *Chinese Chem. Letters* **2005**, *16*, 1467–1470.
[15] M. B. Francis, E. N. Jacobsen, *Angew. Chem.* **1999**, *111*, 987–991; *Angew. Chem. Int. Ed.* **1999**, *38*, 937–941.
[16] C. Marchi-Delapierre, A. Jorge-Robin, A. Thibon, S. Ménage *Chem. Commun.* **2007**, 1166–1168.
[17] a) F. G. Gelalcha, B. Bitterlich, G. Anilkumar, M. K. Tse, M. Beller, *Angew. Chem.* **2007**, *119*, 7431–7435; *Angew. Chem. Int. Ed.* **2007**, *46*, 7293–7296; b) F. G. Gelalcha, G. Anilkumar, M. K. Tse, M. Beller, Abstract of papers from the *234th ACS National Meeting & Exposition*, *Boston*, *MA*, August 19–23, **2007**.
[18] a) D. Yang, M.-K. Wong, Y.-C. Yip, X.-C. Wang, M.-W. Tang, J.-H. Zheng, K.-K. Cheung, *J. Am. Chem. Soc.* **1998**, *120*, 5943–5952; b) I. Moretti, G. Torre, *Tetrahedron Lett.* **1969**, *10*, 2717–2720.
[19] Z.-L. Wei, Z.-Y. Li , G.-Q. Lin, *Tetrahedron* **1998**, *54*, 13059–13072.
[20] Y. Gao, J. M. Klunder, R. M. Hanson, H. Masamune, S. Y. Ko, K. B. Sharpless, *J. Am. Chem. Soc.* **1987**, *109*, 5765–5780.
[21] A. Vidal-Ferran, A. Moyano, M. A. Pericàs, A. Riera, *J. Org. Chem.* **1997**, *62*, 4970–4982.
[22] Z.-X. Wang, Y. Tu, M. Frohn, J.-R. Zhang, Y. Shi, *J. Am. Chem. Soc.* **1997**, *119*, 11224–11235.
[23] The use of *tert*-amyl alcohol as the solvent was found to be unsuitable for the ESIMS measurements.
[24] a) M. L. Ferreira, *Macromol. Biosci.* **2003**, *3*, 179–188; b) M. R. Bukowski, S. Zhu, K. D. Koehntop, W. W. Brennessel, L. Que, Jr., *J. Biol. Inorg. Chem.* **2004**, *9*, 39–48; c) M. Costas, M. P. Mehn, M. P. Jensen, L. Que, Jr., *Chem. Rev.* **2004**, *104*, 939–986.
[25] M. Newcomb, *Tetrahedron* **1993**, *49*, 1151–1176.
[26] a) X.-K. Jiang, *Acc. Chem. Res.* **1997**, *30*, 283–289; b) C.-J. Liu, W.-Y. Yu, C.-M. Che, C.-H. Yeung, *J. Org. Chem.* **1999**, *64*, 7365–7374.
[27] a) H. B. Kagan, *Oil & Gas Science and Technology Rev. IFP* **2007**, *62*, 731–738; Gas Science and Technology Rev. IFP **2007**, 62, 731–738; b) H. B. Kagan, *Synlett* **2001**, 888–899; c) C. Puchot, O. Samuel, E. Dunach, S. Zhao, C. Agami, H. B. Kagan, *J. Am. Chem. Soc.* **1986**, *108*, 2353–2357.
[28] For recent leading references, see: a) W. Nam, *Acc. Chem. Res.* **2007**, *40*, 522–531; b) X. Shan, L. Que, Jr., *J. Inorg. Biochem.* **2006**, *100*, 421–433; c) J. T. Groves, *J. Inorg. Biochem.* **2006**, *100*, 434–437; d) A. Decker, M. D. Clay, E. I. Solomon, *J. Inorg. Biochem.* **2006**, *100*, 697–706; e) I. V. Korendovych, S. V. Kryatov, E. V. Rybak-Akimova, *Acc. Chem. Res.* **2007**, *40*, 510–521; f) R. Mas-Ballesté, L. Que, Jr., *J. Am. Chem. Soc.* **2007**, *129*, 15964–15972; g) S. H. Lee, J. H. Han, H. Kwak, E. Y. Lee, H. J. Kim. , J. H. Lee, S. N. Lee, Y. Kim, C. Kim, *Chem. Eur. J.* **2007**, *13*, 9393–9398; h) F. J. Small, S. A. Ensign, *J. Biol. Chem.* **1997**, *272*, 24913–24920; i) V. Champreda, N. Y. Zhou, D. J. Leak, *FEMS Microbiol. Lett.* **2004**, *239*, 309–318.
[29] J. E. McMurry, *Chem. Rev.* **1989**, *89*, 1513–1524.
[30] S. Chandrasekhar, Ch. Narsihmulu, S. S. Sultana, N. R. Reddy, *Org. Lett.* **2002**, *4*, 4399–4401.
[31] D. Xue, Y.-C. Chen, X. Cui, Q.-W. Wang, J. Zhu, J.-G. Deng, *J. Org. Chem.* **2005**, *70*, 3584–3591.
[32] "30%" aqueous H_2O_2 (Merck) was used as received. The peroxide content varied considerably (0 to 40%), as determined by titration; 50% H_2O_2 was obtained from Aldrich.
[33] Origin 7.5 SR5 [v 7.5870 (B870)] see: https://www.originlab.com/.
[34] A. O. Huque, *Pak.J. Sci. Res.* **1967**, *19*, 140–145.

Received: March 31, 2008
Published online: June 20, 2008

